5th International Conference on Water Resources and Arid Environments (ICWRAE 5): 292-305
7-9 January 2013, Riyadh, Saudi Arabia

The Use of Geophysical and Remote Sensing Data Analysis in the Groundwater Assessment of El Qaa Plain, South Sinai, Egypt

[1]Sultan Awad Sultan,
[2]Nehal Abdel Rahman and [2]Talaat M. Ramadan

[1]National Research Institute of Astronomy and Geophysics, Helwan, Cairo, Egypt
[2]National Authority for Remote Sensing and Space Sciences, (NARSS), Cairo, Egypt

Abstract: In this contribution, different remote sensing and geophysical tools such as geoelectric, magnetic and gravity have been applied to detect groundwater potentiality and structural elements in the study area. Landsat ETM+ image proved to be useful in surface mapping of lithologic and structural features in that area. SRTM images showing enhanced subsurface structures such as faults and paleo-drainages that control the geometry of the groundwater aquifers in the study area. These features are not observable in Landsat ETM+ images of similar resolution. The hydrological analyses of DEM extracted the drainage networks pattern, determined the flow direction of the main channels and find the relationship between paleochannels and structure elements. The results of the quantitative interpretation used to construct six geoelectrical cross-sections indicate that the subsurface sequence of the study area consists of seven geoelectrical units. One hundred and twelve gravity and magnetic stations were measured and interpreted. These studies reveal that the study area was dissected by different fault elements of trends E-W, NW-SE, NE-SW and the E-W trend is mostly control the geometry of the groundwater aquifers in the study area Groundwater data indicated an E-W flow and an increase in salinity towards the Gulf of Suez. The Piper diagram indicates that the water type of the El Qaa Plain is Na-Ca-Cl-SO4 and the hydraulic conductivity of the aquifer 50 m/day. The calculated effective porosity is about 43.1 %. This study demonstrates the utility of use remote sensing and geophysical data for exploring groundwater in the Arabo Nubian Shield and similar regions.

Key words: Gravity · Magnetic · Resistivity · Aquifer · Groundwater · Sinai

INTRODUCTION

The study area, is located between Lat. 28°00` and 28° 40`N and Long. 33° 20` 33° 55` E and extends for some 90 km along the southern section of the eastern coast of the Gulf of Suez (Fig.1). It is bounded to the east by the outskirts of the rugged mountainous area of south Sinai and to the north by Wadi Feiran. Sinai Pensula is a structure defined by the rifts of the Gulf of Suez and the Gulf of Aqaba. It is geographically distinct from both Africa and Asia but serves as a connection between them. Sinai has been the only land bridge between the two continents throughout the Quaternary [1].

Several authors [2-4] have studied the stratigraphic succession of the study area. They indicated that the succession includes, generally rocks ranging in age from Paleozoic to Quaternary. The Quaternary aquifer is composed of gravel, sand, silt and clay. Cobble and boulder-size rock debris of Pre-Cambrian rocks are dominant at the eastern part of El Qaa Plain, while the percentage of carbonates and evaporites of Pre-Quaternary sediments increases at the western side.

Most of the geophysical work [5-11] previously carried out in the study area, was of the purpose of exploring oil potentiality. This included mainly gravity, aeromagnetic and seismic exploration.

The aim of the present work is to elucidate the geology and characterize the Quaternary fresh water aquifer using remote sensing and geophysical processed data and extensive field studies.

Corresponding Author: Sultan Awad Sultan, 1National Research Institute of Astronomy and Geophysics, Helwan, Cairo, Egypt. E-mail: sultan_awad@yahoo.com

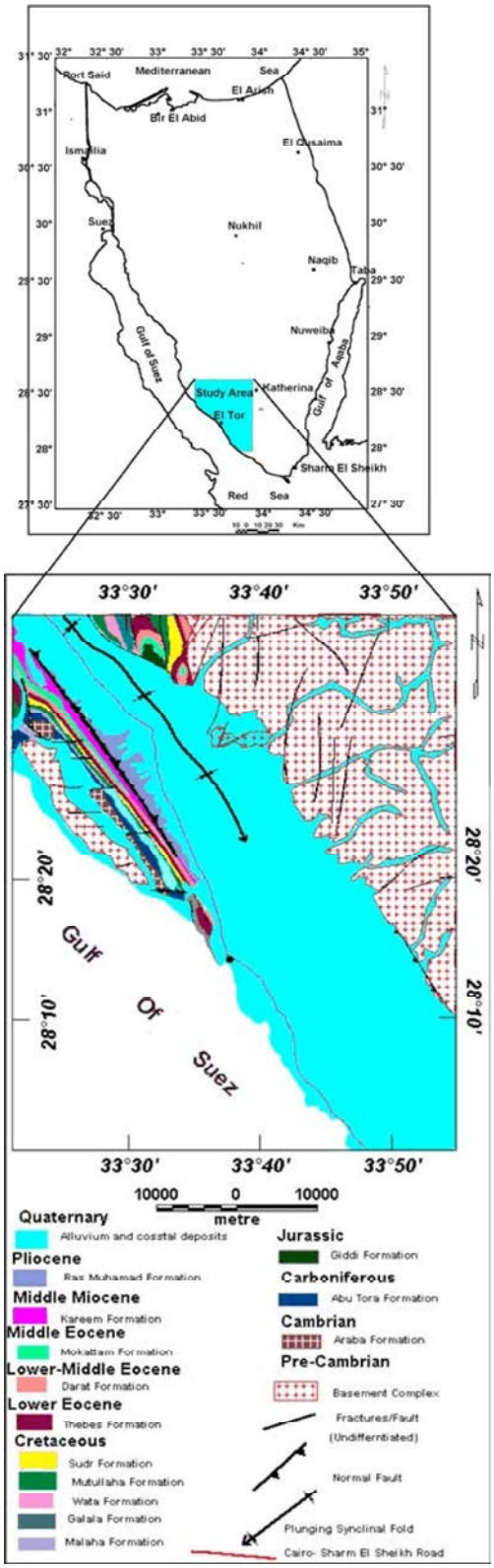

Fig. 1: Location and geological map of the study area (Modified after NARSS and EGSMA [22])

MATERIALS AND MATHODS

Remote Sensing Data: Two sets of remote sensing data were used, the first is the Landsat ETM+ image and the second is the SRTM data. One Landsat ETM+ images (Path: 175, Row: 40) acquired on October 2010. This image has been geometrically and radiometrically corrected. Three bands (7, 4, 2) have been selected, since they contain most of the information about the surface geological features of the study area (Fig. 2a).

The spatial resolution is 30 x 30 m and the image size is 1841x 1869 pixels. The image was processed using the ERDAS Imagine, version 8.3 software, on a Sun spark workstation.

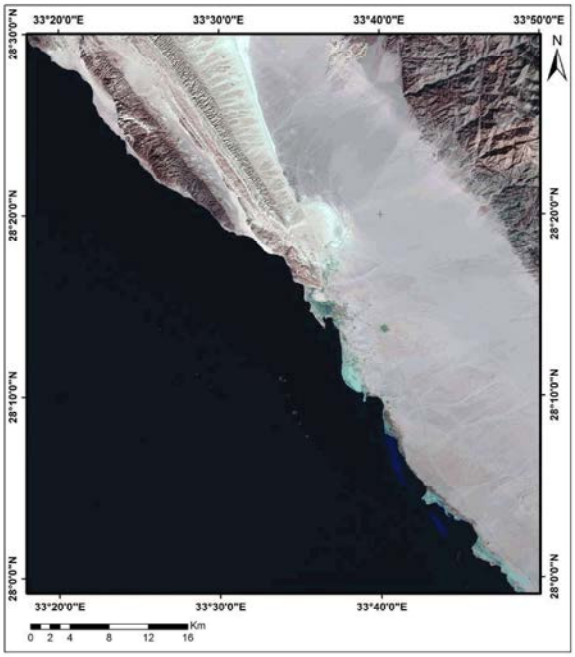

Fig. 2a. Landsat ETM+ image for the study area

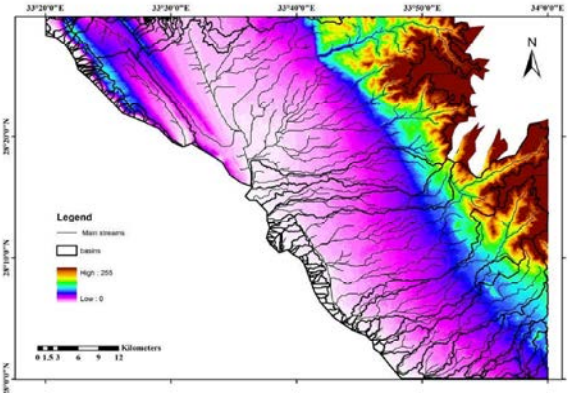

Fig. 2b: The DEM of SRTM for the study area

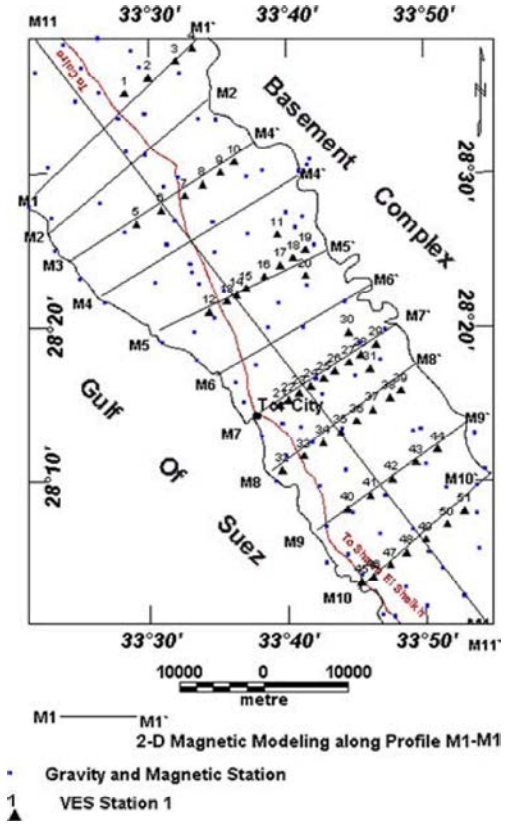

Fig. 3: Geophysical measurements of the study area

The second set is the Shuttle Radar Topography Mission (SRTM) which distributed by the USGS EROS Data Center (EDC) on a near-global scale as part of an international project by the National Geospatial-Intelligence Agency (NGA) and the National Aeronautics and Space Administration (NASA). The STRM data were used to image the paleochannels underneath the recent sand sheets. This is due to the penetration capabilities of radar signals (50 cm for C-band ($\lambda = 5.7$ cm)). The DEM of SRTM was processed to automatically extract the drainage networks pattern, determine the flow direction of the main channels and find the relationship between paleochannels and structure elements (Fig.2b). The hydrological analyses of DEM were carried out using the widely used D-8 algorithm embedded in ArcInfo software with some modifications in the filling of DEM step.

Geophysical Methods: Different geophysical tools including geoelectric, gravity and magnetic have been applied to detect ground-water potentiality and structural elements, which controlled the geometry of the groundwater aquifer in the study area.

Magnetic Data Measurements: Measurements were undertaken at 112 ground magnetic stations (Fig. 3) using an Envimag Proton Magnetometer with a 1 nT sensitivity. The magnetic measurements were corrected for diurnal variations and normal gradient (IGRF). The base station recorded the data every minute while a second station was used as a field instrument. The values of IGRF were calculated at every field station and the values of diurnal variations and IGRF subtracted.

Gravity Data Measurements: An automatic gravity meter made by Scintrex (CG-3 Autograv) with resolution of 0.01 mGal was used to obtain measurements at 112 stations used for the magnetic measurements. Different corrections were applied to the raw data to allow for such factors as drift, tide, latitude, free-air and Bouguer corrections. Terrain correction was also carried out, using the 1:50,000 scale topographic maps to estimate the mean elevation in different zones. The gravity anomalies observed in the Bouguer field are caused by lateral density contrasts within the sedimentary section, crust and sub-crust of the earth.

Geoelectrical Measurements: Fifty-one vertical electrical soundings (VES) were carried out using the Schlumberger configuration with an AB/2 spacing ranging from 1.5m to 1000 m (Fig. 3). The main objective was to detect the Quaternary aquifer and the different sub-surface successions. There are several methods for VES data interpretation: graphical (manual) and analytical methods. The authors used a graphical interpretation, which depends upon matching the plotted field curves with the standard curves and the generalized Cagniard graphs [12]. The results obtained were used as initial model for the analytical methods. The quantitative interpretation was made using the IPI2WIN Program, which deals with VES curves in man-computer interactive regime and draws theoretical and field curves on a display screen together with a Rho(z) model curve.

Description of the Study Area: El Qaa Plain rises up to 200m above sea level (asl), sloping gently towards the south east of the peninsula. It is characterized by young Tertiary and Quaternary alluvial sediments, sandstone, gypsum and limestone. Most of the alluvial sediments originated from the hills to the east [13].

Geomorphologically, the study area can be divided into three geomorphological units: i) High relief mountains of basement rocks which rise to 2662 m asl at Gabal Katherine in the east, b) The western part consists of the Gabel Qabilat and Gabel Arabah hills which are generally between 200 and 300 m asl and composed of different sedimentary units and basement rocks, c) The majority of the area consists of wadi deposits, rock fragments, alluvium deposits (sand and gravel), sabkha and playa, ranging from 0 to 200 m asl.

The subsurface stratigraphy was obtained from the El Qaa-1 Well, drilled in the central part of the study area [14]. This borehole indicated presence of sand, gravel and boulders to a depth of 6m, below which sand and gravel was present to 23 m, sand and gravel with clay intercalations to 40 m, sand to 54 m, sand and gravel with clay intercalations to 105 m and sand with clay intercalations to the bottom of the borehole at 110 m.

Structurally, the Gulf of Suez is the northwestern arm of the Red Sea rift system which is bounded by a major border extensional fault [15]. The El Qaa Plain is a secondary rift basin. Most of the wadis dissecting the basement complex are straight and narrow with steep walls, indicating a structural control.

Hydrogeologically, the eastern margin of the aquifer consists of sandy gravel and gravelly sand, typical of alluvial fan deposits with a high hydraulic conductivity (about 50 m/day) while the coastal area, consisting mainly of limestone, coral reefs and clay alternating with continental sabkha and alluvial deposits has a lower hydraulic conductivity about 5 m/day [3]. The rate of groundwater extraction has increased from about 500 m3/day in1930 [16] to about 26000 m3/day in 2000 [3]. The aquifer divided into three distinct zones with hydraulic gradients about 0.00395, 0.006 and 0.000775. The salinity of the water in the El Qaa Plain under natural conditions varies due to differences in recharge conditions, intensity of flow and lithology. The fresh water zone (TDS up to 800 mg/l) is associated with the best recharge and hydraulic conductivity conditions while in the coast area heavy abstraction via dug wells has resulted in an increase in salinity increased from about 1000 to 10000 mg/l [3].

RESULTS AND DISCUSION

Geology of the Study Area: False colour Landsat TM images (Bands 7,4,2 in R, G, B) of the study area was used for surface lithological and structural analysis. The field studies indicated that the investigated area is mostly covered by Quaternary deposits which consist of alluvium, sabkha and costal sand, representing the El Qaa Plain deposits (Fig. 1). The eastern and northeastern parts of the study area are occupied by different geological units ranging from Precambrian to Pliocene in age as following:

- The Pliocene consists of highly fossiliferous reefal limestone (the Ras Muhamed Formation).
- The Middle Miocene is represented by interbedded anhydrite and limestone of the Kareem Formation.
- The Middle Eocene includes a yellowish white chalky limestone with a few chert concentrations (the Mokattam Formation) below which is the Middle-Lower Eocene (Darat Formation)-a greyish-white limestone with marl and claystone. The Lower Eocene is represented by the Thebes Formation, a grey to white compacte limestone.
- The Cretaceous includes five separate Formations: the Sudr (white to gray chalk), Mutullah (agillaceous limestone and marl with shale), Wata (limestone intercalated with sandstone and shale), Galala (marl and claystone) and Malaha (sandstone intercalated with mudstone).
- The Jurassic deposits are represented by the marl, limestone and clay of the Giddi Formation.
- The Carboniferous deposits are represented by the Abu Tora Formation which consists of sandstone with fossiliferous clayey beds.
- The Cambrian deposits include the varicolored sandstone and sandy claystone of the Arabah Formation.
- Granitic Precambrian basement rocks occupy the eastern part of the study area and the northeastern part of Gabal Arabah.

The geological map indicates two normal faults, in the western (F1) and eastern (F2) parts of the site. In the northern part of the El Qaa Plain there is a pronounced syncline plunging southeastwards (Fig. 1)

The DEM of SRTM: The hydrological analyses of DEM extracted the drainage networks pattern, determined the flow direction of the main channels and find the relationship between paleochannels and structural elements as follows:

- The drainage pattern drained from the surrounding highlands and drain westerly into an internal lowland area basins and having the NNE trend (Fg. 2b).

- The Stream Definition function takes a flow accumulation grid as input and creates a Stream Grid for a user-defined threshold. Two thresholds have been used to create the main buried streams for the whole watershed (Fig. 2b). These indicate that the direction of water flow from southwest toward the Gulf of Suez.
- The Catchment processing function generates the aggregated upstream catchments from the "Catchment" feature class (Fig. 2b). They are divided into several basins and these basins follow the main surface catchment areas.
- The study area was dissected by different fault elements of trends E-W, NW-SE, NE-SW and the E-W trend which mostly control the geometry of the groundwater aquifers in the study area.

Magnetic Data Interpretation: The corrected magnetic values were represented on a map with contour intervals of 10 nT using the Geosoft Program [17]. The resulting picture represents a preliminary total intensity magnetic map (Fig. 4). It can be seen that there are high magnetic anomalies in the eastern, northwestern and southern parts of the area while the central part has low magnetic anomalies. The sources of the magnetic anomalies (basement rocks) are exposed in the eastern and northeastern parts of the study area. The final picture is the total intensity map reduced to the pole (Fig. 4). This map was used for magnetic interpretation (eg 2-D magnetic modeling) in order to estimate the depth of the basement rocks.

The magnetic response of the subsurface geological sections was calculated using 2-D magnetic modeling along 11 profiles (Fig. 3), ten of which have a NE-SW direction while M11 is NW-SE. A magnetic susceptibility of 0.000750 cgs units and magnetization (m) of 0.00398 emu/cm^3 were used to construct the 2-D magnetic models based on the El Qaa-1 well. The basement rocks are within a few meters of the surface in the western side of the study area, increasing to a maximum depth of 2,615 m in the central part of the area (profiles M1 to M5). The depths estimated from profiles M6 to M11 varied from 650 m at beginning of the profile to 1,400 m at the centre of the profile and rising again to c. 600 m at the end of the profile. In M11, the basement rocks are again very shallow at the beginning (about 50 m), increasing to 1,400 in at the central part then rising to 300 m before dropping to 1,500 m at the end of the profile (Fig. 5). The basement relief map constructed from the 2-D modeling is shown in Fig. (6).

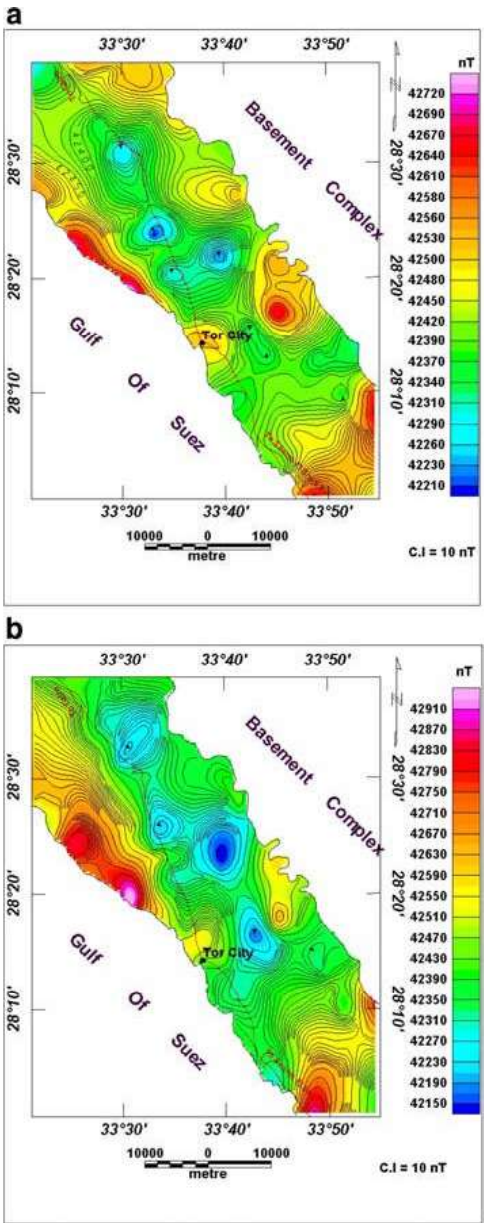

Fig. 4: a) Total intensity magnetic map, b) total intensity magnetic map reduced to the pole

Gravity Data Interpretation: Based on the corrected gravity data, a Bouguer anomaly map (Fig. 7) was constructed using Geosoftw Program [17]. For regional residual gravity separation, there are many different techniques for gravity separation. In the present work [8] least-squares method has been applied to separate the regional component (Z) from the Bouguer anomaly (Fig). The residual component (R) can be estimated as follows:

$$R = \Delta g - Z \quad (1)$$

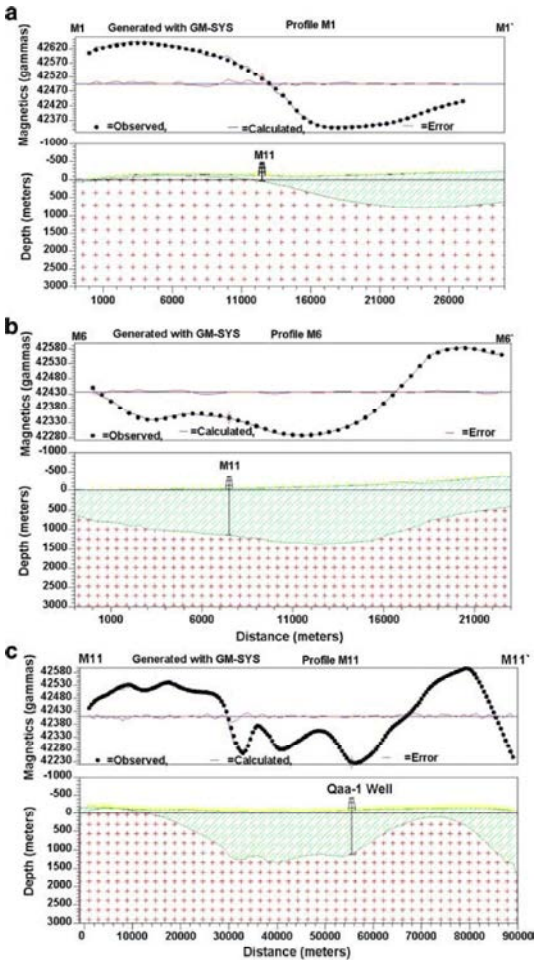

Fig. 5: a) 2-D magnetic modeling along profile M1-M1°, b) 2-D magnetic modeling along profile M6-M6°, c) 2-D magnetic modeling along profile M11-M11°

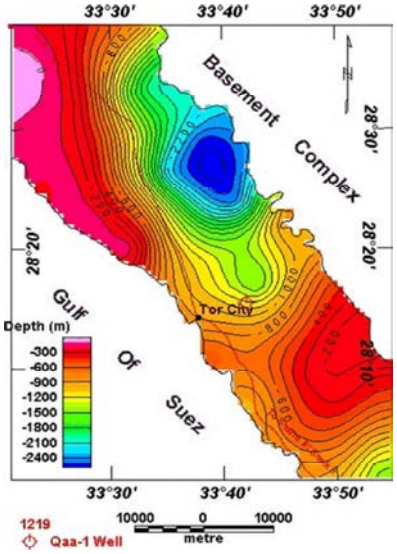

Fig. 6: Basement relief map of the study area

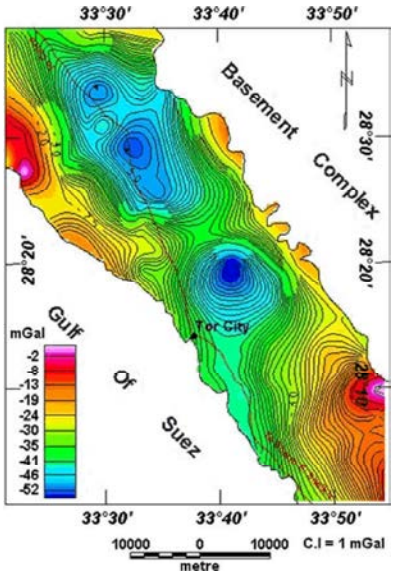

Fig. 7 Bouguer anomaly map of the study area

In all cases, the condition of the least-squares solution is

$$\sum R^2 = \text{minimum}$$

The regional surface is represented by polynomial [18-20] as given by the following equation:

$$Z(x,y) = \sum_{n=0}^{p} \sum_{s=0}^{n} a_{n-s,s} x^{n-s} y^{s} \qquad (2)$$

Where the $\alpha_{n\text{-}s,s}$ are l/2(p + l)(p + 2) coefficients and p is the order of the two-dimensional (2-D) polynomial; x and y are the coordinates.

In the present work the calculations were carried out to the 5th order. The residual component has been estimated by subtracting regional values (Z) from Bouguer values (Fig). The results of separation of regional and residual for different orders were mapped by Geosoft Program [17]. Figures 8a-e and Figures 9a-2 represent the regional and residual components for the first to fifth orders respectively. A correlation factor r(x,y) has been calculated to select the best order of residual for gravity interpretation. The correlation factor can be estimated for any two orders, such as between i-and j-orders for residual (rij),

$$r(x,y) = \frac{\sum xy - \frac{(\sum x)(\sum y)}{2}}{\sqrt{\left[\left(\sum x^2 - \frac{(\sum x^2)}{n_x}\right)\left(\sum y^2 - \frac{(\sum y^2)}{n_y}\right)\right]}} \qquad (3)$$

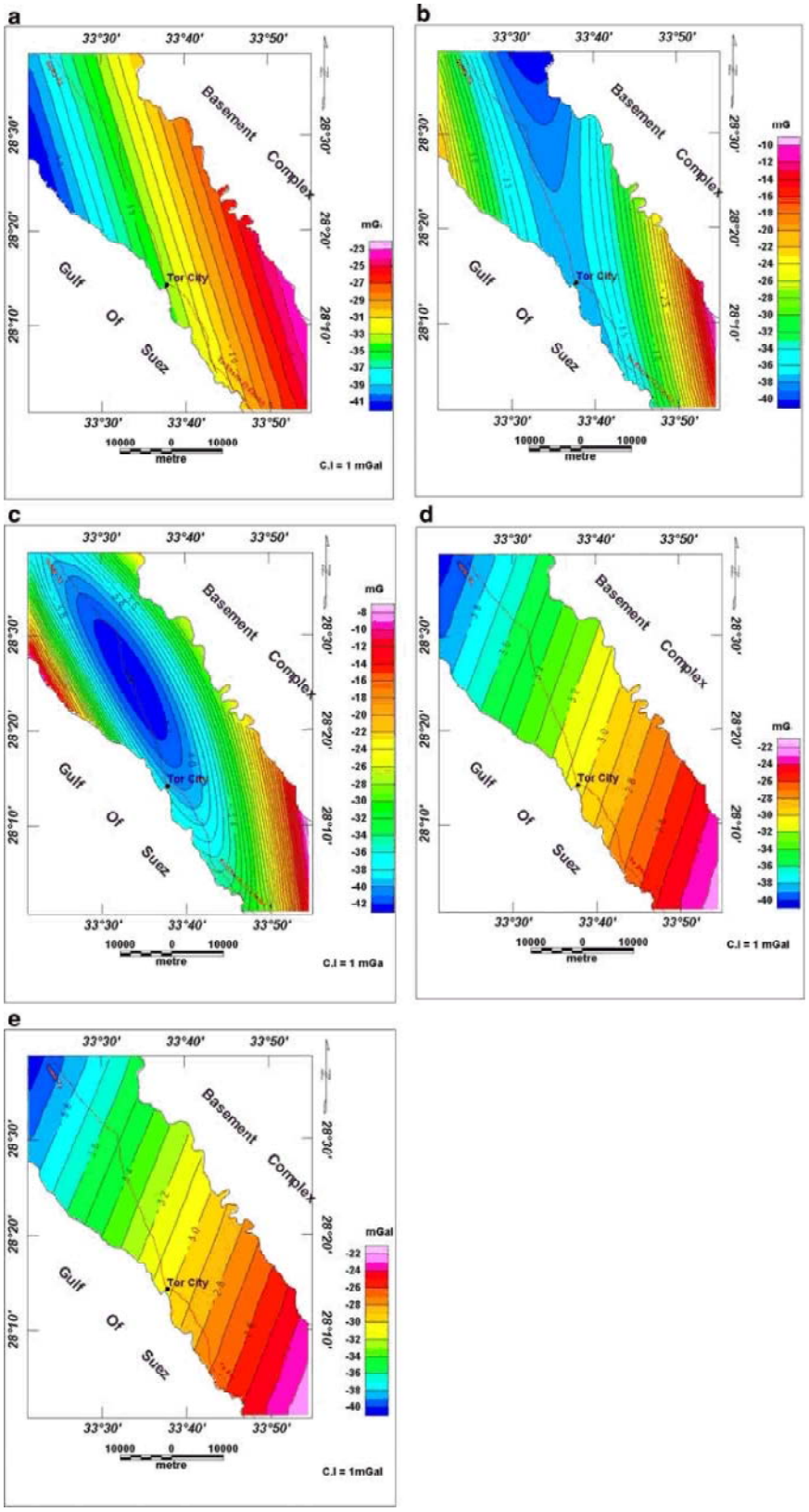

Fig. 8: Regional gravity map: a) first order, b second order, c) third order, d) fourth order and e) fifth order

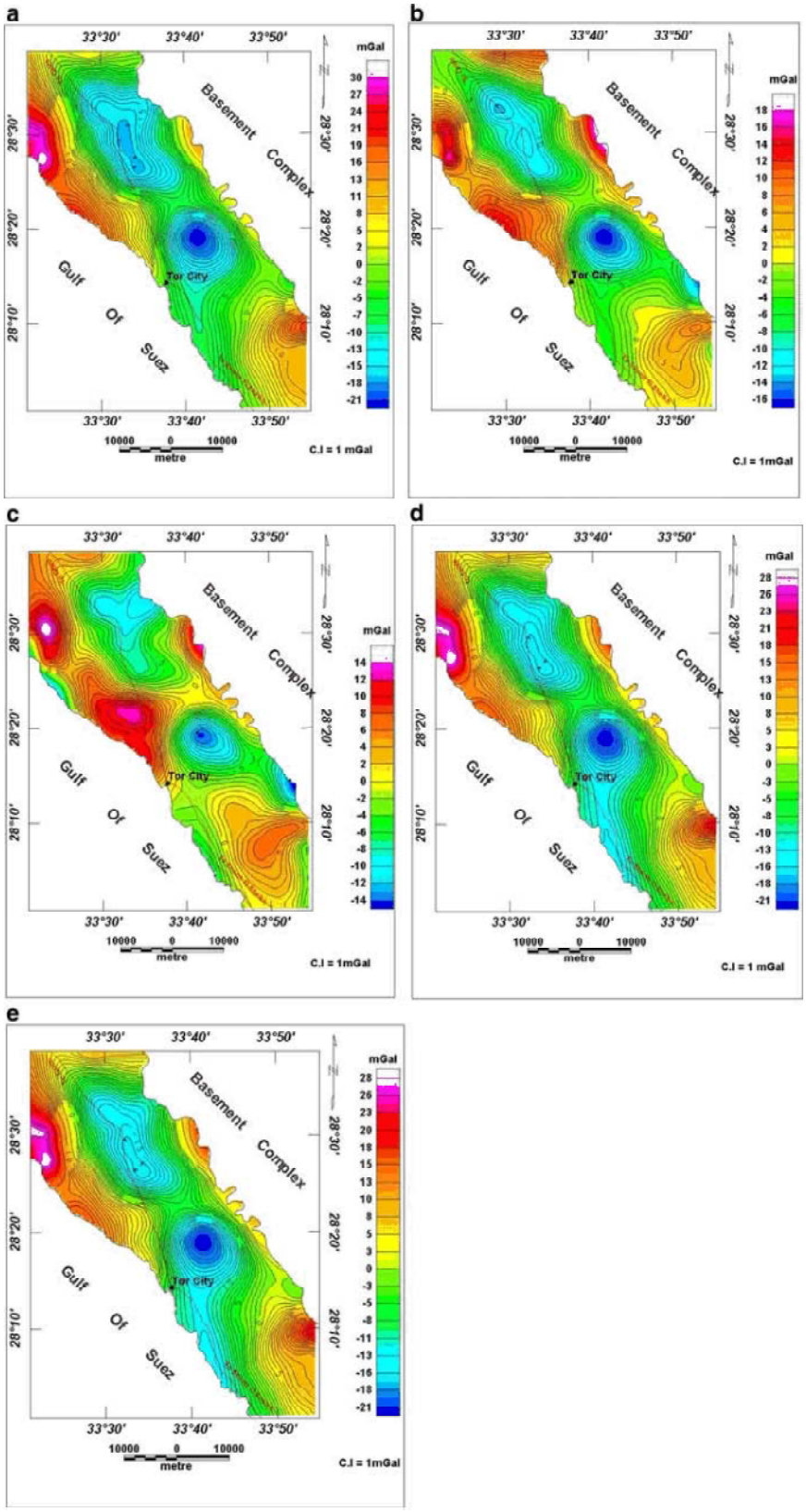

Fig. 9: Residual gravity map: a) first order, b) second order, c) third order, d) fourth order and e) fifth order.

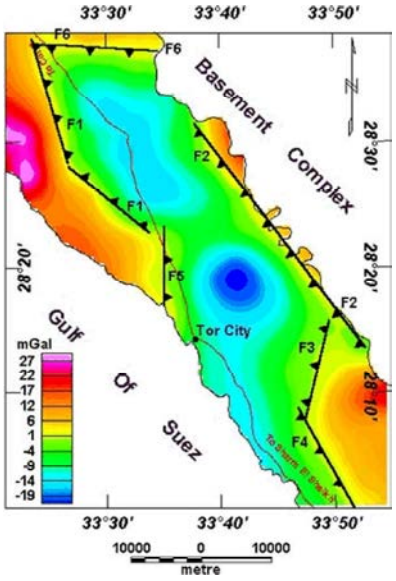

Fig. 10: Fault elements dissecting the study area from gravity

The results are given in Table (1), from which it can be seen that the fourth order (R_{45}) is the best for gravity interpretation.

A fourth order residual gravity anomaly map was used to detect the location and trends of the faults dissecting the study area. This map (Fig. 10) indicates that the eastern part of the study area is dissected by faults F1 and F5; the upper part of the F1 can be traced on surface (Fig. 1) with a NNW-SSE trend, consistent with that of the Gulf of Suez. Fault F5 has a N-S trend, parallel to the Nile Valley and downthrows towards the east. Fault F2 is also shown on the geological map near the eastern boundary of the site, to the western side of the basement rocks. The southern part of the study area is dissected by faults F3 and F4; F3 with a trend similar to the Gulf of Aqaba and F4 similar to the Gulf of Suez. The northern part is dissected by E-W fault F6.

Geoelectrical Interpretation: The geoelectrical quantitative interpretation has been applied to determine the thicknesses and true resistivities of the stratigraphic units below each VES station and in the construction of seven geoelectrical cross-sections as following:

- The geoelectrical cross-section along profile1, in the northern part of the study area, includes four VES stations. Geological unit beneath VES 1 and 2 is the gravel and boulders of high resistivity that overlie the relatively shallow El Qaa aquifer units. These have a thickness of 60 m and consist of sand and gravel of moderate resistivity (26-28 ohm.m) and sand and gravel with clay intercalations which show low resistivity (8-14 ohm.m). The aquifer overlies the Pliocene reefal limestone deposits with high resistivity, below which are the low resistivity (7 ohm.m) Middle Miocene clastic sediments with anhydrite. There is a normal fault (F6) located near VES station 3 which separates the Miocene and Quaternary deposits (Fig. 11a).
- The geoelectrical cross-section along profile 2 (Fig. 11b) exhibits a deeper (about 50 m) and thicker (about 200 m) Quaternary aquifer; the lower surface detected at VES station 9 being at 257 m depth. This aquifer is also divided into two units; the upper unit has moderate resistivity (14-147 ohm.m) and the lower unit exhibits low resistivity (4-15 ohm.m).
- The thickness of the Quaternary deposits is increased at the geoelectrical cross-section along profile 3 (Fig.11c), where the depth of the aquifer is deeper than in profiles 1 and 2 (31-84 m); the lower surface was not detected. There is a normal fault (F1) located between VES stations 12 and 13, separating the Middle Eocene and Quaternary deposits.
- The geoelectrical cross-sections along profiles 4, 5, 6 and 7 (Figs. 11d, 11e, 11f and 11g) indicated a similar situation with two units in the Quaternary aquifer trough, although the lower surface of the aquifer was not detected in the western parts of the profiles. Cross-sections 6 and 7 are dissected by faults F4 and F5 respectively.

The results of the VES interpretation were used to construct isoresistivity, depth maps and isopach maps for the upper part of Quaternary aquifer. The isoresistivity map (Fig. 12a) indicates that the true resistivities decrease from east to west. The eastern part is near the wadis which dissect the basement rocks and represents the recharge zone. This is reflected in the increased resistivity (55-90 ohm.m) at the fresh water bearing zone compared with the higher resistivities due to salinization of the groundwater towards the west and south. Figure (12b) indicates that the depth of the aquifer increases gradually eastward from few meters to 80 m. The isopach map (Fig. 12c) indicates the thickness of the upper unit of the aquifer (the fresh water component consisting of gravel and sand) increases gradually from 20 m in the north to 100m in the eastern part of the central area.

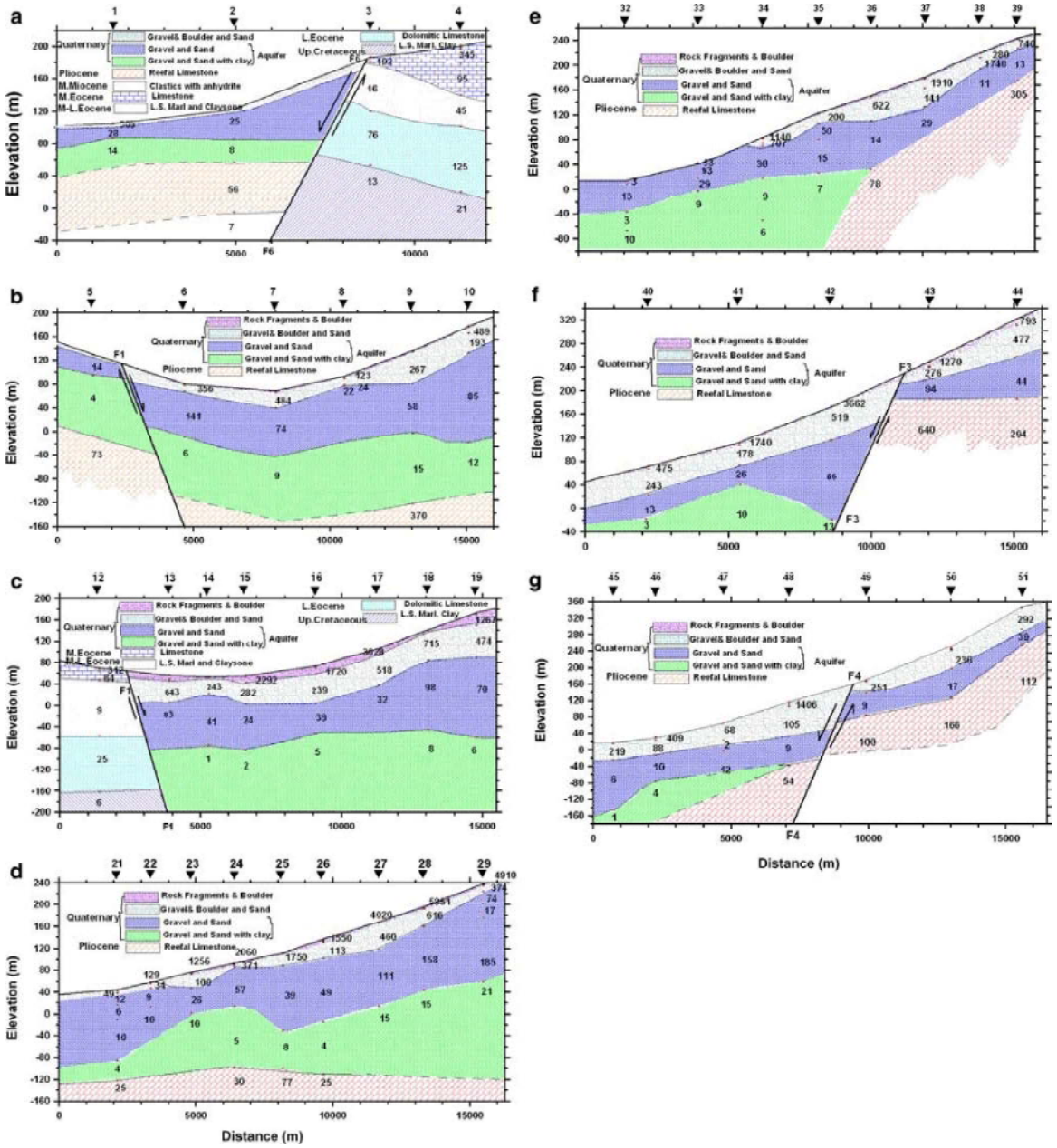

Fig. 11: Geoelectrical cross-section along profiles 1, 2, 3, 4, 5, 6 and 7

Hydrogeology: The eastern margin of the Quaternary aquifer consists of sandy gravel and gravelly sand, typical of alluvial fan deposits with a high hydraulic conductivity (about 50 m/day) while the coastal area, consisting mainly of limestone, coral reefs and clay alternating with continental sabkha and alluvial deposits [3], has a lower hydraulic conductivity (about 5 m/day). The rate of groundwater extraction has increased from about 500 m^3/day in1930 [16] to about 26000 m^3/day in 2000 [3]. The aquifer has been divided into three distinct zones with hydraulic gradients about 0.00395, 0.006 and 0.000775. The salinity of the water in the El Qaa Plain under natural conditions varies due to differences in recharge conditions, intensity of flow and lithology. The fresh water zone (TDS up to 800 mg/l) is associated with the best recharge and hydraulic conductivity conditions while in the coast area heavy abstraction via dug wells has resulted in an increase in salinity from about 1000 to 10000 mg/l.

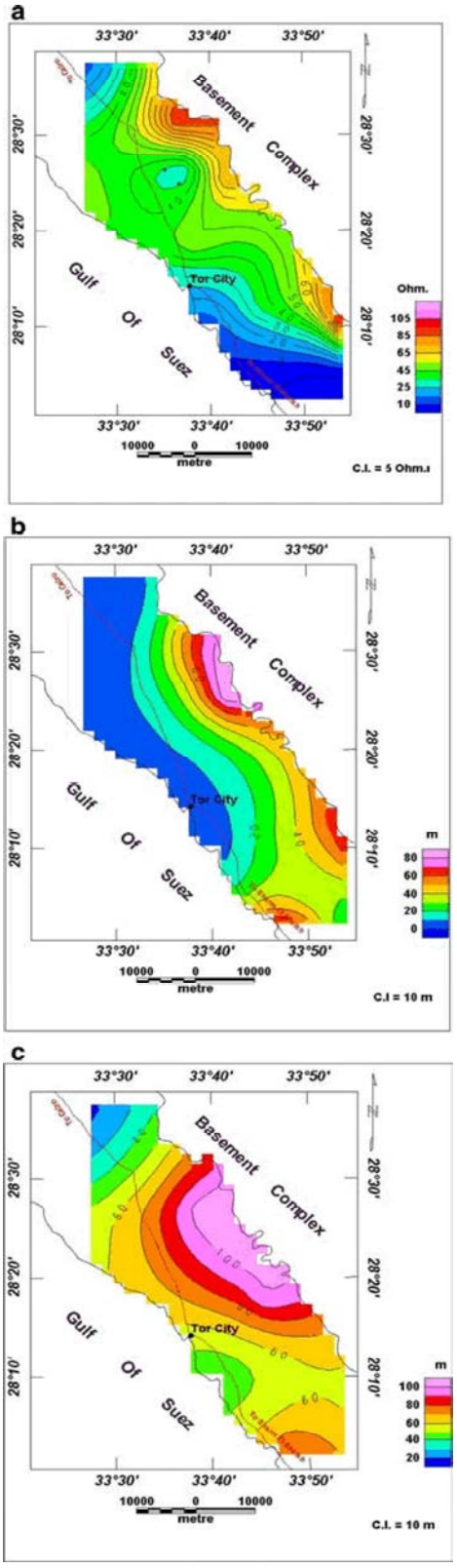

Fig. 12: a) Isoresistivity map, b) depth map of the aquifer, c) Isopach map of the upper unit of El Qaa aquifer

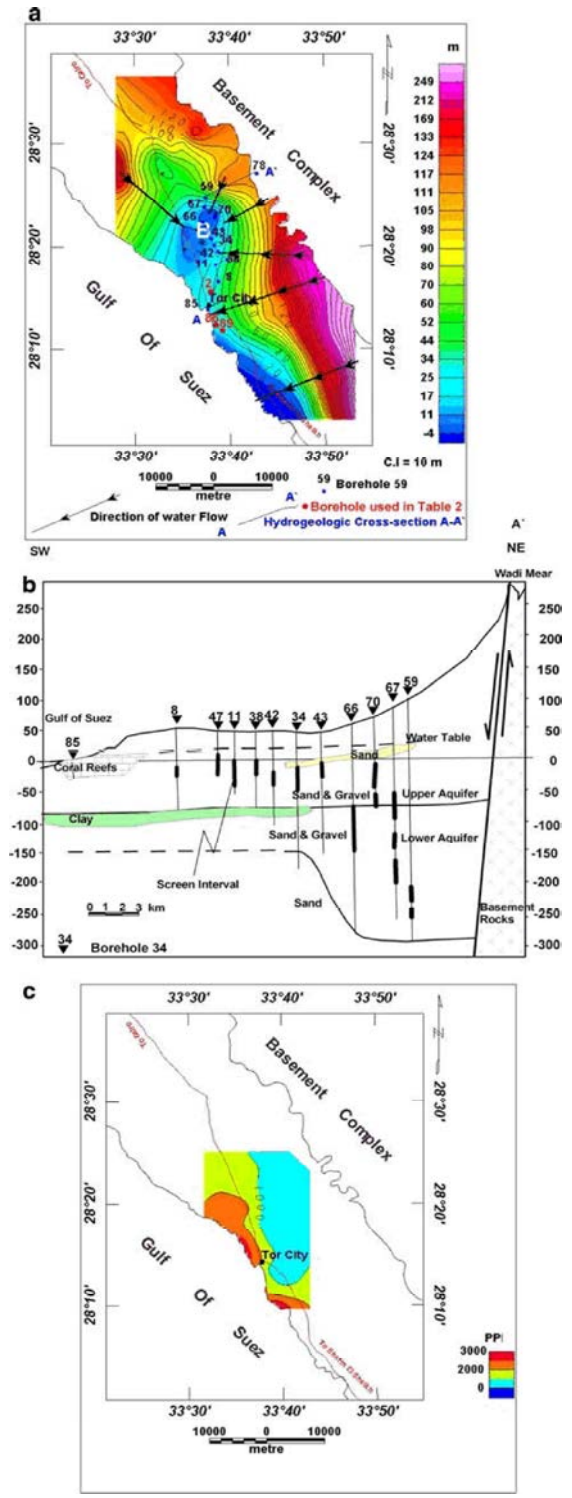

Fig. 13: a) The water table map constructed from interpreted geoelectrical data, b) Hydrogeological cross-section A-A° modified after Ghodeif and Groski 2001, c) salinity map (modified after Gorski and Ghodeif 2000 and Sayed *et al*. 2004)

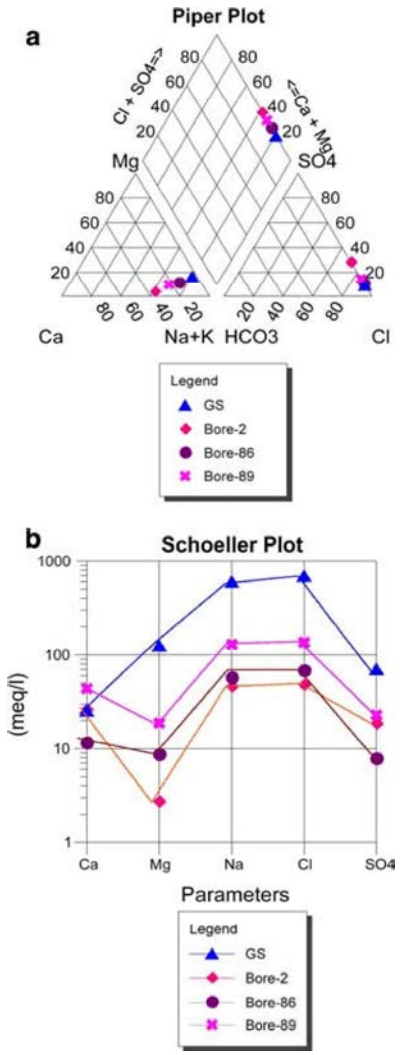

Fig. 14: Piper diagram and Schoeller diagram to detect water type

The water table map (Fig. 13a), constructed from interpreted geoelectrical data, indicates the elevation of the water table decreases from the east and north towards the west. The productive boreholes are concentrated at zone B, where the water table is at about 10 m depth. The water flow direction is southwest, towards the Gulf of Suez. Hydrogeological cross-section A-A` was constructed using borehole data from [21]. This includes a group of boreholes located in the central part of the area and starts from A at Gulf of Suez to A` at Wadi Mear (Fig. 13b). This section again indicates that the aquifer consists of an upper and lower aquifer, with thicknesses decreasing from east to west. A normal fault is shown between he basement rocks and Quaternary aquifer.

The salinity map was based on hydrochemical analysis for total dissolved salts (TDS) for the boreholes reported by [3] and [14]. The central part of the area has fresh and brackish water with TDS values ranging from 500 to 3000 ppm (Fig. 13c).

Porosity Calculation: The effective porosity (Φ_{eff}) was calculated from the hydraulic conductivity of 50 m/day estimated by [3] and Marotz's equation:

$$\Phi_{eff} = 25.5 + \ln(k) \quad (4)$$

Where the Φ_{eff} equals 43.1 %

Water Type: From the hydrochemistry obtained in some of the boreholes reported by Gorski and Ghodeif (2000), the type of water was assessed by plotting the data on the Piper trilinear diagram and the ratios of the main ions using the Schoeller diagram (Fig. 14). This indicated that the water type is Na-Ca-Cl-SO4 and the ratios of ions are higher for the Gulf of Suez water (GS) and the lower Bore-2. The salinization of the groundwater is calculated through the REX factor-{(Na+K+Mg in meq/l)-1.076 Cl}. The negative values in GS, Bore-2 and Bore-89 indicate salinization in these boreholes which are near the Gulf of Suez and suffering sea water intrusion, while the positive value in Bore-86 indicates fresher ground water.

CONCLUSIONS

From the results of the remote sensing and geophysical data interpretation as well as the geological and hydrogeological studies of the area, it is concluded that:

- Landsat ETM+ images proved to be useful in surface mapping of lithologic and structural features in that area. SRTM images reveal fluvial features beneath a surface cover of the desert sand for the first time in the northern and western parts of the study area. These features are not observable in Landsat ETM+ images of similar resolution. Radar images showing enhanced subsurface structures such as faults and paleo-drainages that control the geometry of the groundwater aquifers in the study area.
- The hydrological analyses of DEM extracted the drainage networks pattern, determined the flow direction of the main channels and find the relationship between paleochannels and structural elements.

- The study area contains a Quaternary aquifer which can be divided into two units: an upper unit composed of gravel and sand of moderate resistivity, which reflects fresh water condition and a lower unit composed of gravel and sand with clay intercalations and brackish water.
- The best recharge and hydraulic conductivity conditions are in the eastern part of the aquifer where high quality ground is found. The direction of water flow is southwest, towards the Gulf of Suez; the salinity of the water increased in this direction.
- The area is dissected by a series of faults trending NW-SE, NE-SW, N-S and E-W, related to the regional structural trends of Gulf of Suez, Gulf of Aqaba, Nile Valley and Mediterranean Sea respectively. The E-W trend mostly control the geometry of the groundwater aquifer in the study area.
- The thickness of the sedimentary deposits increases from a few meters in the northwestern part of the study area to 1200 m in the south and 2615 m in the centre.
- The type of water is Na-Ca-Cl-SO4

The study demonstrates the utility of integrating optical and radar remote sensing and geophysical data for exploring groundwater in the Arabo Nubian Shield and similar regions.

REFERENCES

1. Tchernov, E., 1979. The fauna: meeting point of two continents. In Sinai: Pharaohs, Miners, Pilgrims and Soldiers, by B. Rothenberg and H. Weyer. Washington, DC: Binns, pp: 93-99.
2. Webster, D.I. and N. Riston, 1992. Post-Eocene Stratigraphy of the Suez rift in South-west Sinai, Egypt. E.G.P.C., Sixth Exploration Seminar, Cairo, March, 1992, 1: 276-288.
3. Gorski, J. and K. Ghodeif, 2000. Salinization of shallow water aquifer in El Qaa coastal plain, Sinai, Egypt. In: Proceedings of 16th salt water intrusion meeting, Wolin Island, Poland.
4. Leppard, C.W. and R.L. Gawthorpe, 2006. Sedimentology of rift climax deep water systems; Lower Rudeis Formation, Hammam Faraun Fault Block, Suez Rift, Egypt. Sediment. Geol., 191: 67-87.
5. Geofizica, 1963. Final report, southwestern Sinai, reconnaissance investigations, hydrogeology, geophysics and soil studies.Zagreb, Yugoslavia, pp: 184.
6. Kamel, H. and A. Fouad, 1975. Project of establishing the gravity map of Egypt, Bouger map, scale 1,500,000. G. P. C. Co., Egypt.
7. Shendy, E.H., 1984. Geological and geophysical investigation for groundwater in El Qaa Plain, Southwestern Sinai. M. Sc. Thesis, Faculty of Science, Suez Canal University, Ismailia.
8. Abdelrahman, E.M., E. Refai and Y. Amin, 1985. On least-squares residual anomalies determination, Geophysics, 50(3): 473-480.
9. Tealeb, A. and S. Riad, 1987. Regional tectonic of Sinai Peninsula interpreted from gravity and deep data. In: EGS Proceedings of 5th annual meeting, pp: 18-49.
10. Meshref, W.M. and M.I. El-Kattan, 1989. Tectonic pattern of El Qaa Plain, Sinai Development, Ismailia, Egypt, pp: 33-42.
11. Ibrahim, S. and A.A. Ghoneimi, 1992. A contribution of the potential field data to establish the subsurface configuration of the southwestern Sinai, Egypt. In: Proceedings of 3rd conference on geology and Sinai development, Suez Canal University, Ismailia, Egypt.
12. Koefoed, O., 1960. A generalized Cagniard graph for interpretation of geoelectric sounding data, Geophysical Prospecting, 8(3): 459-469.
13. Monier, M., M. Abd El-Ghani and M.A. Wafaa, 2003. Soil-vegetation relationships in a coastal desert plain of southern Sinai, Egypt, Journal of Arid Environments, 55: 607-628.
14. Sayed, M.A., M.A. El-Fakharany and M.F. Hamed, 2004. Integrated geophysical and hydrogeological studies on the Quaternary aquifer at the middle part of El Qaa Plain, SW Sinai, Egypt, Egyptian Geophysical Society. EGS J., 2(1): 135-145.
15. Said, R., 1990. Geology of Egypt. Balkema, Rotterdam, pp: 722.
16. Attia, M.A., 1930. Report on fresh water of El Tor Quarry. Unpublished report, Geol. Surv. Of Egypt, pp: 11 (in Arabic).
17. Oasis Montaj, 2007. Geosoft mapping and application system, Inc, Suit 500, Richmond St. West Toronto, ON Canada N5SIV6.
18. Oldham, C. and D.B. Sutherland, 1955. Orthogonal polynomials, their use in estimating the regional effect: Geophysics, 20: 295-306.

19. Grant, F.S., 1957. A problem in the analysis of geophysical data. Geophysics, 22: 309-344.
20. Van Voorhis, G.D. and T.M. Davis, 1964. Magnetic anomalies North of Puerto Rico: Trend removal with orthogonal polynomials: J. Geophys. Res., 69: 5363-5371.
21. Ghodeif, K. and J. Gorski, 2001. Protection of fresh ground water in El Qaa Quaternary aquifer, Sinai, Egypt. New Approaches characterizing Flow, Seiler and Wonhnlich, Swets and Zeitliger Lisse, ISBN 902651 848 X.
22. NARSS and EGSMA, 2004. Geologic Map of Sinai, Egypt, Scale 1:500,000. Geological Survey of Egypt.